Proc. 2002 Australasian Conference on Robotics and Automation
Auckland, 27-29 November 2002

Sensing Airflow by a Humanoid Robot

R. Andrew Russell
Intelligent Robotics Research Centre, Monash University, Clayton, VIC 3800
andy.russell@eng.monash.edu.au

Abstract

This paper describes the development of a system for measuring airflow moving past the head of a humanoid robot. In recent years there has been growing interest in the development of humanoid robots. To function in a safe and efficient manner a humanoid robot must be 'aware' of its surroundings. For both a human and a humanoid robot airflow can provide useful information. Airflow sensors measure local air movement and can detect such things as draughts resulting from open doors and the air disturbance caused by walking close to the humanoid robot. When used in conjunction with an odour sensor measurements of airflow in the vicinity of a humanoid robot can also provide important information for localising the source of an odour. This paper describes progress in the development of an airflow measuring system that is compatible with the humanoid form and gives results showing that it can indicate both airflow velocity and direction.

1 Introduction

For human beings the human form is of intrinsic interest and a lot can be learnt about human function through building humanoid robots. Particularly in Japan there is considerable interest developing humanoid robots with the ability to walk [Hirai, *et al.*, 1998], [Kagami, *et al.*, 2000]. Having human proportions gives many advantages to a robot designed to operate in a human world, to interact with humans or to assist the aged or infirm. As well as having a human form, it can be argued that humanoid robots should also have similar sensory awareness to that of a human. This will allow the robot to operate safely in a human environment. The human environment is relatively unstructured and contains many unpredictable hazards that must be detected. In addition, a robot acting as a carer for the elderly or ill patient may need to provide substitute sensory capabilities to help compensate for the failing eyesight, hearing, smell, touch, etc. for the people under its care.

The senses appropriate for a humanoid robot are usually considered to be the five classical human senses of vision, touch, hearing, taste and smell [Dario, *et al.*, 1997]. Of these sensing modalities vision has received the most attention. However, to maintain an awareness of its surroundings a humanoid robot will require a rich set of sensory clues. While the detection of local airflow does not fit any of the five classical human senses it can provide important environmental information. Draughts caused by open doors and windows can be detected and localised. As people walk about they push a ‘bow wave’ of disturbed air ahead of them. The proximity of people approaching from any angle can be detected by observing the resulting airflow. Airflow is usually involved in the distribution of chemical stimuli because diffusion is impossibly slow at normal robot scales. A smouldering electrical fire, the wearer of a sumptuous perfume, a leaking gas pipe, can all be located by olfactory sensing and in many cases knowledge of the local airflow helps to track down the source. The mechanism for sensing odour is quite different from the more usual forms of robotic sensing such as vision and laser/ultrasound ranging. Chemical sensors only measure concentration at the location of the sensor. They are not directional and do not form images. To locate the source of a chemical plume knowledge of the local airflow is required in order to 'project' chemical sensor readings towards the source. In the Intelligent Robotics Research Centre at Monash

University a humanoid robot is being developed [Price, *et al.*, 2000] and airflow sensing whiskers are one of its sensory systems. Figure 1 shows the plastic head created for the humanoid robot by Dr Andrew Price, together with the airflow sensing whiskers mounted on a headband. On the table in front of the robot is an electronic nose that is also being developed for the humanoid robot [Purnamadjaja and Russell, 2000]. This paper describes the design of the sensory whiskers and provides some preliminary results from these devices. In the future it is planned to combine data from the airflow sensing whiskers and electronic nose in order to detect, identify and determine the source of odours.

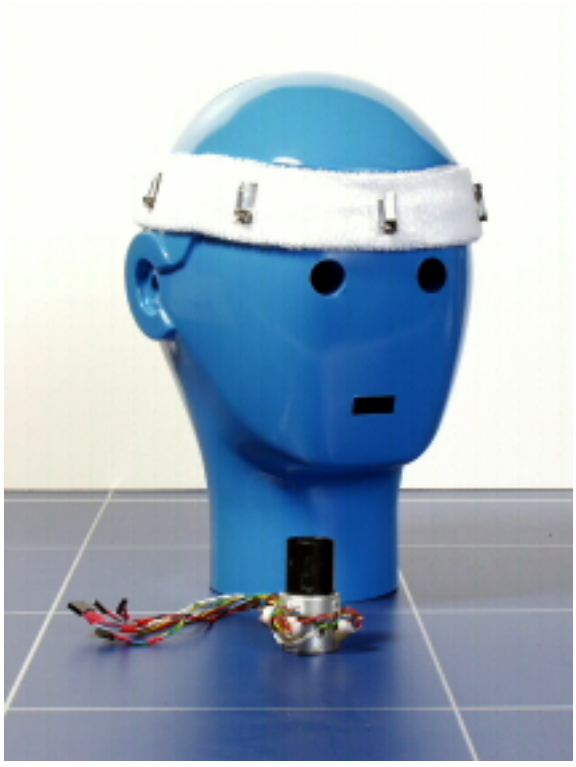

Figure 1 A photograph of the humanoid head with airflow sensing whisker attached to a headband.

2 Measuring airflow

Many methods of measuring airflow such as wind turbines and hot wire anemometers do not work well at low velocities . For robotics applications a novel windvane has been developed by Russell and Kennedy [Russell and Kennedy, 2000]. However, this consisted of a rotating paddle that would not be compatible with the humanoid form. In order to measure airflow in a non-intrusive manner it was decided to investigate one of the techniques that humans use for detecting airflow. At least two mechanisms provide information about airflow. The skin on the face can give a statistically significant sensation for changes of 0.001˚C/sec [Geldard, 1972]. Therefore it seems reasonable to assume that the cooling effect of airflow on the skin can indicate wind direction based on the varying velocity of airflow around the head. The side of the head away from the wind will be sheltered and therefore less cooling will indicate a lower velocity. An alternative effect is the disturbance of fine body hairs caused by fluctuations in the airflow passing over the skin. If this turbulence can be detected then it could be used to indicate wind direction as it does in humans. To test this idea the airflow sensing whisker shown in Figure 2 was designed. The sensing element is a 5mm wide strip of aluminised plastic film and vibrations of this strip are detected by an optical sensor. To get a suitable combination of stiffness and dimensional stability 25µm thick PVdF film was used (note that the piezoelectric properties of the film were not employed in this application). A tab formed by putting a 90˚ bend in the end of the whisker interrupted the light beam in a slotted optical switch (Omron type EE-SX1109).

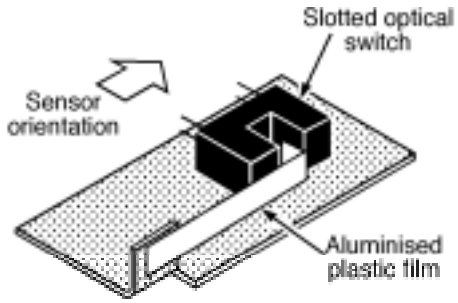

Figure 2 The whisker airflow sensor.

The output of the optical switch was fed into a schmitt inverter to give a signal with a full logic swing. A measured movement of 0.04mm gave a change in logic output of the inverter. Positive going logic transitions were counted by a 68HC12 microcontroller and this count formed the output of the sensor.

The plastic film constitutes a vibrating beam with one end fixed and the other free. The fundamental resonant frequency of the whisker is [Timashenko, *et al.*, 1974]:

$$f_1 = \frac{3.515}{2\pi}\sqrt{\frac{EI}{\rho A l^4}}$$

where:

E = Young'ss modulus ($2*10^9$ N/m^2)

l = beam length (15mm)
A = cross-section area
ρ = material density ($1.78*10^3$ kg/m^3)

the moment of inertia of the beam's cross-section *I* is:

$$I = \frac{bw^3}{12}$$

where:

b = beam breadth (5mm)
w = beam width ($25*10^{-6}$m)

Substituting the whisker's parameters gives a fundamental resonant frequency of 10.8Hz. The resonant frequency measured for one of the whiskers was 31Hz. A major cause of the discrepancy between measured and calculated frequency is believed to be the shape of the whisker cross-section. Distortion of the whisker introduced when cutting the material with a scalpel blade significantly increased the moment of inertia of the cross-section and raised the whisker stiffness and resonant frequency.

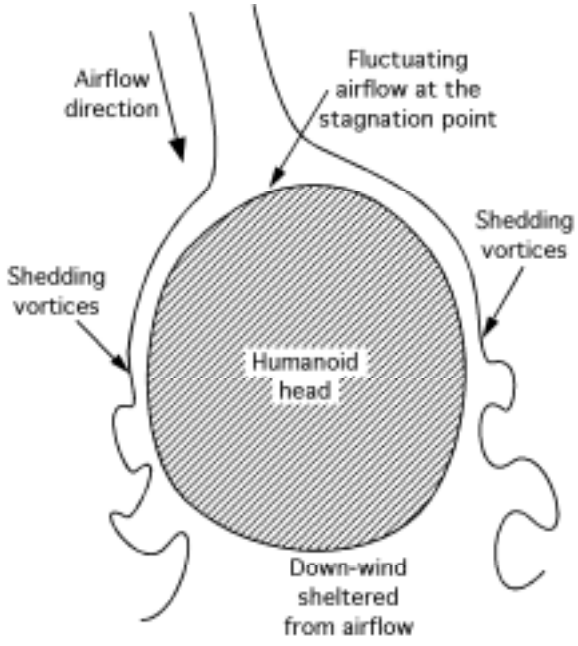

Figure 3 The airflow around the humanoid head.

Fluctuations in the airflow over the whisker that contain a significant component at the whisker's fundamental resonant frequency tend to transfer energy to the whisker and cause it to oscillate. Experimental measurements have shown that there are three main regions where fluctuations in the airflow excites vibrations in the whisker sensors. If the airflow is incident on the head at 0˚ then at points corresponding to angles of 90˚ and 270˚ the air flowing around the head separates from the surface (see Figure 3). At these symmetrical points there is a great deal of fluctuation in the airflow. A stagnation point occurs in the area where the incident airflow meets the head (0˚). In laminar airflow there would be little air movement at this point. However, airflow from the fan was far from steady and these fluctuations were detected by the whisker sensor at this point. The far side of the head (180˚) was sheltered from the airflow and little variation in the airflow was detected. This interpretation agrees with the sensor data plotted in Figure 4.

3 Results

Figure 4 shows whisker sensor measurements spaced every 20˚ around the humanoid head. These measurements were made in an airflow of 0.25m/s approaching the head on a bearing of 0˚. The airflow was created using a domestic cooling fan running from a variable transformer to give control of the fan velocity.

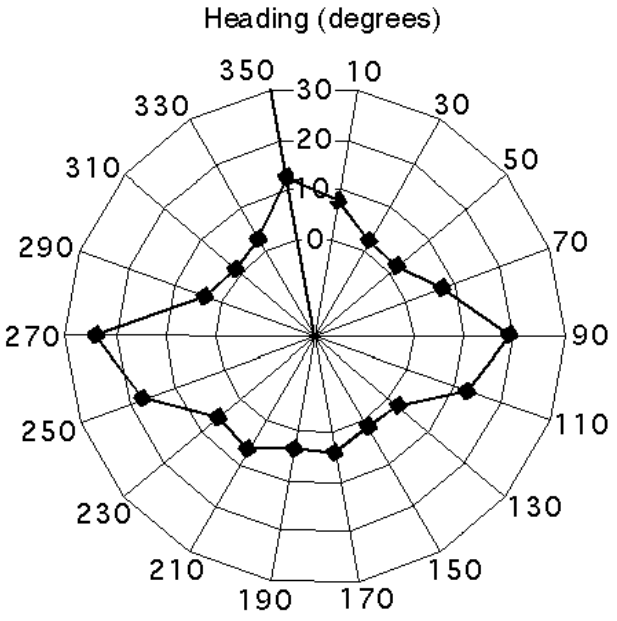

Figure 4 Whisker sensor output in terms of pulses integrated over a 10 second period measured at a wind velocity of 0.25m/s.

At low airflow velocities the magnitude of the whisker sensor output is related to velocity of the airflow. The humanoid head and a turbine anemometer were positioned

2m down wind of a cooling fan. Figure 5 shows the reading on the anemometer and average sensor reading in pulses per second for the whisker sensor positioned at the stagnation point (0˚)versus the fan voltage. A consistent relationship between the anemometer reading and the output of the whisker sensor is seen over the range 0.1m/s to 1.0m/s. The turbine anemometer could not indicate below 0.1m/s. However, the whisker sensor still gave readings at lower fan speeds.

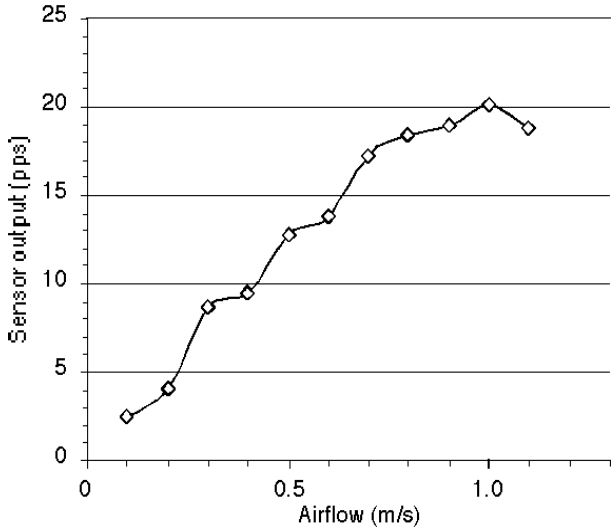

Figure 5 Sensor output positioned at 0 degrees (averaged over 10 seconds) related to airflow velocity.

In order to determine the direction of airflow 8 whisker sensors were mounted on a sweatband worn by the humanoid head (see Figure 1). Two sets of reference readings were taken with the head rotated 22.5˚ to give sensor readings spaced 22.5˚ apart round the head. Airflow was set at 0.45m/s during the reference measurements. In order to calculate the bearing of airflow incident on the head a single measurement x_i was taken from the 8 sensors. This set of readings was then compared with a subset of the 16 reference measurements y_i using correlation. In calculating the correlation C_j where j is the offset the reference elements y_i were found by indexing into the array using the index (j + 2*i) mod 16.

$$C_j = \frac{8\sum_{i=1}^{8} x_i y_i - \sum_{i=1}^{8} x_i \sum_{i=1}^{8} y_i}{\sqrt{\left[8\sum_{i=1}^{8}(x_i)^2 - \left(\sum_{i=1}^{8} x_i\right)^2\right]\left[8\sum_{i=1}^{8}(y_i)^2 - \left(\sum_{i=1}^{8} y_i\right)^2\right]}}$$

The offset j that gave the strongest correlation corresponded to the angle of incidence of the airflow. Figure 6 shows the correlation between sensor readings for an airflow incident at 300˚ and the reference readings. The maximum correlation corresponds to a heading of 315˚.

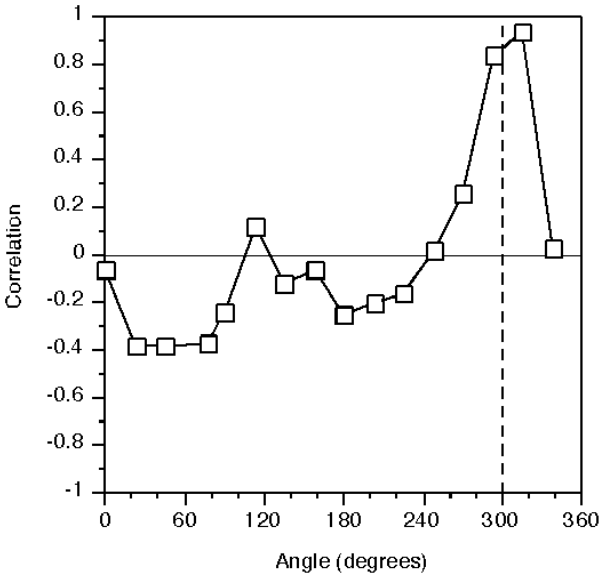

Figure 6 The correlation between a set of reference measurements and readings taken with airflow of 0.35m/s incident at a bearing of 300˚.

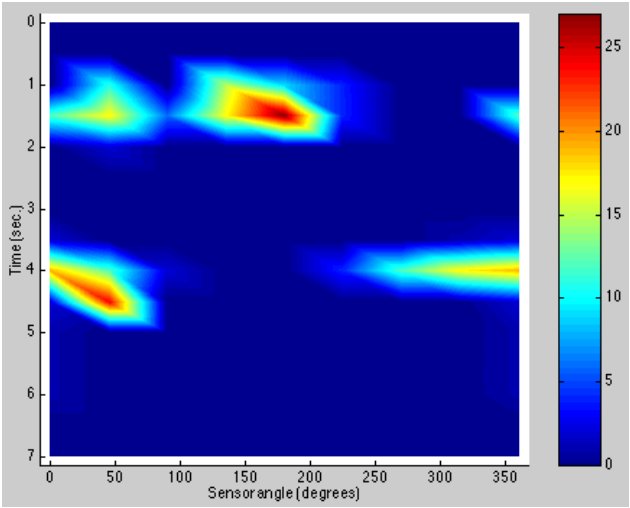

Figure 7 Airflow sensor system response to the wash caused by walking right to left behind the humanoid head and then left to right in front.

In addition to measuring the relatively steady airflow from a cooling fan the whisker sensors also responded to the current of air displaced by walking close to the head.

Figure 7 shows the sensor response to a person walking left to right in front of the humanoid head followed by walking right to left behind the head. In both cases the walker travelled at about 2m/s and passed within one metre of the head. The response of the sensors to the wash did not give a strong correlation with the reference measurements taken in a steady airflow. However, in each of the sets of results shown in Figure 7 there are regions that seem to be sheltered from the disturbed air. Walking right to left behind this region is centred about 290˚ and walking left to right in front 150˚. The regions are almost 180˚ apart and therefore seem to relate to the trajectory of the walker with respect to the head (see Figure 8).

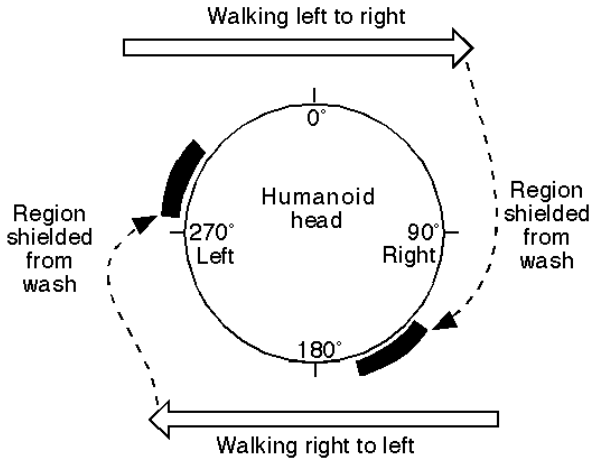

Figure 8 Regions of the humanoid head shielded from the wash of air caused by walking past the head.

4 Conclusions

At Monash University a range of sensor systems are being developed for a humanoid robot [Price, et al., 2000]. An important design consideration is that these sensors blend in with the humanoid form and this has influenced the development of the airflow sensory system that is the subject of this paper. The airflow measuring system consists of 8 whisker sensors attached to a headband worn by the humanoid. This system can be used to measure both wind velocity in the range 0.1m/s to 1m/s and direction in increments of 22.5˚. This sensor system provides information that can be combined with odour readings to indicate the direction to the odour source. The airflow sensor also provides unique information such as the presence of draughts and disturbed air caused by people walking past the robot. In the future, the size of the whisker sensors will be reduced and their resistance to damage will be improved before the whisker sensors and electronic nose are integrated into the humanoid robot head.

Acknowledgments

The author would like to acknowledge helpful discussions with Professor John Sheridan concerning fluid flow. Dr Andrew Price designed and built the plastic shell of the humanoid head. The work reported in this paper is part of a project titled “Robotic Humanoid” that was supported by a SMURF2 grant from Monash University.

References

[Dario *et al.*, 1997] Paolo Dario, Cecilia Laschi, and Eugenio Guglielmelli, ‘Sensors and actuators for ‘humanoid’ robot’, *Advanced Robotics*, Vol. 11, 1997, pp. 567-583.

[Geldard, 1972] Frank, A. Geldard, *The Human Senses: Second Edition*, John Wiley and Sons, Inc., 1972.

[Hirai, *et al.*, 1998] Hirai, K., *et al.*, 'The development of Honda humanoid robot', *Proceedings of the IEEE International Conference on Robotics and Automation*, May 1998, pp.1321-1326.

[Kagami, *et al.*, 2000] Kagami, S., *et al.*, 'Design, implementation, and remote operation of the humanoid H6', *Proceedings of the International Symposium on Experimental Robotics*, December 10-13, 2000, pp. 41-50.

[Price, et al., 2000] Andrew Price, A, *et al.*, 'A lightweight plastic robotic humanoid', *Proceedings of the IEEE/RSJ International Conference on Intelligent Robots and Systems*, Takamatsu, Japan, 2000, pp. 1571-1576.

[Purnamadjaja, and Russell, 2000] Anies, H. Purnamadjaja, and R. Andrew Russell, 'A sense of smell for a humanoid robot', *International Conference on Artificial Intelligence in Science and Technology*, Hobart, Tasmania, 17-20 December 2000, pp. 312-316.

[Russell and Kennedy, 2000] R. Andrew Russell and Stephen Kennedy, 'A novel airflow sensor for miniature mobile robots', *Mechatronics*, Elsevier Science, Vol. 10, No. 8, 2000, pp.935-942.

[Timoshenko, et al., 1974] Stephen Timoshenko, *et al.*, *Vibration Problems in Engineering, Fourth Edition*, John Wiley & Sons, New York, 1974.